Studierendentagung
Lübeck 2014

Proceedings

Student Conference 2014
Studierendentagung 2014
Medical Engineering Science
Medizintechnik
Lübeck, March 12–14, 2014
Lübeck, 12.–14. März 2014

Editors / Hrsg.:
T. M. Buzug, R. Birngruber, H. Botterweck, R. Brinkmann
H. Gehring, H. Handels, H. Hellbrück, C. Hübner, G. Hüttmann
S. Klein, M. Koch, M. Leucker, N. Linz, A. M. Mamlouk
T. Martinetz, A. Mertins, S. Müller, B. Nestler, H. Paulsen
M. Ryschka, A.-P. Schulz, A. Schweikard, R. Rahmanzadeh

BioMedTec Wissenschaftscampus
UNIVERSITÄT ZU LÜBECK
FACH HOCHSCHULE LÜBECK
University of Applied Sciences
Medisert
Technologie- und Wissenstransfer BioMedTec Wissenschaftscampus
Life Science Nord

Bibliographic information published by the German National Library:

The German National Library lists this publication in the National Bibliography; detailed bibliographic data are available on the Internet at http://dnb.dnb.de .

Imprint:

Copyright © 2014 GRIN Verlag
ISBN: 9783656596509

This book at GRIN:

https://www.grin.com/document/268650

T. M. Buzug et al.

Student Conference on Medical Engineering Science

Band 3

Student Conference Medical Engineering Science 2014

Proceedings

GRIN Verlag

Life Science Nord

Jobs with good prospects

Clever heads are looking for Jobs in Northern Germany.

Visit our website:

www.life-science-nord.net/jobs

www.facebook.com/LifeScienceNord

Innovation for your health.

SCHLESWIG-HOLSTEIN, HAMBURG

Exhibitors

OLYMPUS

PHILIPS

MÖLLER-WEDEL INTERNATIONAL
Tradition and Innovation

EUROIMMUN

Fraunhofer MEVIS

stryker

Cooperation Partners

BioMedTec Wissenschaftscampus

UNIVERSITÄT ZU LÜBECK

FACH HOCHSCHULE LÜBECK
University of Applied Sciences

Medisert
Technologie- und Wissenstransfer
BioMedTec Wissenschaftscampus

norgenta
North German
Life Science Agency

Life Science Nord

Land Schleswig-Holstein

Proceedings

Student Conference on Medical Engineering Science 2014

Lübeck, March 12–14, 2014

Conference Chair

Thorsten M. Buzug (Chair), Institute of Medical Engineering, Universität zu Lübeck
Stephan Klein (Co-Chair), Center for Biomedical Technology, University of Applied Sciences Lübeck

Local Coordination

Kanina Botterweck, Medisert, BioMedTec Science Campus
Martina Galler, Medisert, BioMedTec Science Campus
Christian Kaethner, Institute of Medical Engineering, Universität zu Lübeck
Christina Debbeler, Institute of Medical Engineering, Universität zu Lübeck
Gisela Thaler, Institute of Medical Engineering, Universität zu Lübeck

Scientific Program Committee

Reginald Birngruber, Institute of Biomedical Optics, Universität zu Lübeck
Henrik Botterweck, Center for Biomedical Technology, University of Applied Sciences Lübeck
Ralf Brinkmann, Institute of Biomedical Optics, Universität zu Lübeck
Thorsten M. Buzug, Institute of Medical Engineering, Universität zu Lübeck
Hartmut Gehring, Clinic of Anesthesiology, University Medical Center Schleswig-Holstein, Campus Lübeck
Heinz Handels, Institute of Medical Informatics, Universität zu Lübeck
Horst Hellbrück, Center of Excellence CoSA, University of Applied Sciences Lübeck
Christian Hübner, Institute of Physics, Universität zu Lübeck
Gereon Hüttmann, Institute of Biomedical Optics, Universität zu Lübeck
Stephan Klein, Center for Biomedical Technology, University of Applied Sciences Lübeck
Martin Koch, Institute of Medical Engineering, Universität zu Lübeck
Martin Leucker, Institute for Software Engineering and Programming Languages, Universität zu Lübeck
Norbert Linz, Institute of Biomedical Optics, Universität zu Lübeck
Amir Mandany Mamlouk, Institute for Neuro- and Bioinformatics, Universität zu Lübeck
Thomas Martinetz, Institute for Neuro- and Bioinformatics, Universität zu Lübeck
Alfred Mertins, Institute for Signal Processing, Universität zu Lübeck
Stefan Müller, Center for Biomedical Technology, University of Applied Sciences Lübeck
Bodo Nestler, Center for Biomedical Technology, University of Applied Sciences Lübeck
Hauke Paulsen, Institute of Physics, Universität zu Lübeck
Ramtin Rahmanzadeh, Institute of Biomedical Optics, Universität zu Lübeck
Martin Ryschka, Laboratory for Medical Electronics, University of Applied Sciences Lübeck
Arndt-Peter Schulz, Laboratory for Biomechanics and Biomechatronics, Universität zu Lübeck
Achim Schweikard, Institute for Robotics and Cognitive Systems, Universität zu Lübeck

Preface and Acknowledgements

After the great success of the first meetings in 2012 and 2013, the 3rd Student Conference on Medical Engineering Science 2014 shows a steady growth in quality and quantity of scientific contributions. The experienced organization team of the BioMedTec Science Campus Lübeck in cooperation with Norgenta, the North German Life Science Agency, has spared no effort to provide a wonderful conference, where master students of the campus present their recent research results to a broad public of academics and industry. The contributions show how physics, engineering and computer sciences can advance medicine, health and health care. Moreover, this conference offers a good opportunity for both students and companies to get in touch at the industrial exhibition and to get to know each other from a different point of view.

Students from the Life Sciences programs at the BioMedTec Science Campus present their results from projects carried out at the laboratories and institutes of Lübeck's Universities, in international research facilities and research-oriented industrial companies. The conference focus has been placed on topics from medical engineering. This interdisciplinary field has been established at the University of Applied Sciences Lübeck for decades and Medical Engineering Science (Medizinische Ingenieurwissenschaft – MIW) is an important bachelor and master program at the Universität zu Lübeck as well. Both universities jointly offer the international master degree course Biomedical Engineering (BME). This is complemented with further life science oriented programs of the University (Computer Sciences, Medical Computer Sciences, Mathematics in Medicine and Life Sciences, Molecular Life Science, Medicine) which contribute to the success of the Medical Engineering Science and Biomedical Engineering programs.

I want to thank all the people who worked with enthusiasm and dedication to make the conference a successful event. Without the financial support of Norgenta and the State of Schleswig-Holstein, this conference would not have been possible. I have to thank the companies who support the meeting. Moreover, my thanks go to the technology transfer platform Medisert of the BioMedTec Science Campus. The professional management of Kanina Botterweck and her Medisert team has contributed substantially to the success of this conference. Personally and on behalf of all colleagues of the BioMedTec Science Campus, I especially want to thank Christian Kaethner and Christina Debbeler from the Institute of Medical Engineering. They have been the first contact point for all questions of students and the program committee members. Their in-depth overview of all details of this event is the key to the success of the 3rd Student Conference at the BioMedTec Science Campus.

Lübeck, March 12–14, 2014

Prof. Dr. Thorsten M. Buzug
Vice President of the Universität zu Lübeck
Chair of the 3rd Student Conference
on Medical Engineering Science 2014

Contents

Biochemical Optics I

Biochemical Optics II

Biochemical Physics

Biomedical Engineering I

Biomedical Engineering II

Signal Processing

Imaging and Image Computing I

Imaging and Image Computing II

Magnetic Resonance Imaging I

Magnetic Resonance Imaging II

LUMEN

1
Biomedical Optics I

Improving the stability of an interferometry-based photoacoustic detection

A. Auner, J. Horstmann, C. Buj and R. Brinkmann

***Abstract*–This paper deals with the improvement of the interferometric stability for a photoacoustic measurement system. In this system, pressure induced surface displacement in the nanometer range are measured by the use of Electronic Speckle Pattern Interferometry (ESPI). Because the system suffers from high vibrational noise, the mechanical noise sources are evaluated in the presented paper. In order to improve the stability of the system, several investigations have been carried out. Main causes of the noise are the vibration of the laser chiller, the tube which transfers the vibrations to the lab bench and the irregular water flow. By optimizing these conditions , the noise is reduced from ±40 nm to ±8 nm, which is a suitable stability for the use of the system in photoacoustic imaging.**

I. Introduction

At the Medical Laser Center Luebeck (MLL), a non-contact photacoustic imaging approach is developed, in which the deformation of a laser stimulated volume surface is detected by an additional illumination laser in an interferometric setup [1]. This approach enables photoacoustic detection in 2 D with acquisition times far below one second. From the displacement data, a photoacoustic tomography can be calculated [2]. However, the new system suffers from poor mechanical stability which is necessary to detect the desired very small surface displacements in nm range. In order to investigate the mechanical stability and noise sources, a Mach-Zehnder-Interferometer (Fig. 1) which detects optical path length differences between the object beam and a reference beam is realized. If there are vibrations in the system, this influences the measurement. The setup is operated using the same components and is located on the same table compared to the photoacoustic detection setup, so the results can be transferred.

At the start of the investigations, the chiller for the laser (Edgewave BX6IE, wavelength 532 nm, pulse duration <10 ns, repetition rate 1 Hz – 5 kHz) is located right under the lab bench. For the detection a high speed camera (Photron SA3-120k, CMOS chip, Pixel Size 17 µm, resolution 1024² Pixels) is used, which can be operated in a range of 100 Hz to 5 kHz.

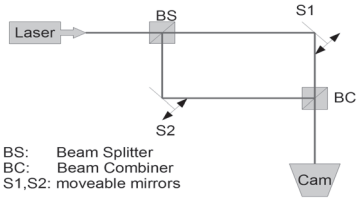

Fig. 1: Mach-Zehnder interferometer

The interferometer is adjusted to the highest contrast, where the path lengths for the beam are equally. From the measured interferograms, phase changes of subsequent images are acquired are by the use of the Spatial Phase Shifting Electronic Speckle Pattern Interferometry (SPS ESPI) method [3]. Using this method, the object and reference beam have to interfere under an angle which results in a phase gradient β over the detector, which is given by

$$\beta = \frac{2\pi}{NP} \qquad (1)$$

NP is the number of adjacent pixels within 2π. The intensity in each pixel is

$$I_{ges} = I_{ref} + I_{obj} + 2\sqrt{I_{ref} * I_{obj}} * \cos(\alpha + \Delta\varphi) \qquad (2)$$

To solve these equation after φ, two additional phases are added. For NP=3, β has 120° so Δφ=0°, Δφ=120° and Δφ=240°.

$$I_1 = I_{ref} + I_{obj} + 2\sqrt{I_{ref} * I_{obj}} * \cos(\alpha + 0) \qquad (3)$$

$$I_2 = I_{ref} + I_{obj} + 2\sqrt{I_{ref} * I_{obj}} * \cos(\alpha + 120) \qquad (4)$$

$$I_3 = I_{ref} + I_{obj} + 2\sqrt{I_{ref} * I_{obj}} * \cos(\alpha + 240) \qquad (5)$$

The phase difference between object beam and reference beam can be calculated by solving the equation system:

$$\Delta\varphi = \arctan\left(\frac{\sqrt{3}(I_1 - I_3)}{2I_2 - I_1 - I_3}\right) \qquad (6).$$

A. Auner, Medizinische Ingenieurwissenschaft, Universität zu Lübeck; the work has been carried out at the Medical Laser Center Luebeck GmbH, Luebeck, Germany (e-mail: auner@miw.uni-luebeck.de)

J. Horstmann is with the Medical Laser Center Luebeck GmbH, Luebeck, Germany (e-mail: horstmann@mll.uni-luebeck.de)

C. Buj is with the Institute of Biomedical Optics, Universität zu Lübeck, Luebeck, Germany (e-mail: buj@bmo.uni-luebeck.de)

Dr. R. Brinkmann is with the Medical Laser Center Luebeck GmbH, Luebeck, Germany and the Institute of Biomedical Optics, Universität zu Lübeck, Luebeck, Germany (e-mail: brinkmann@mll.uni-luebeck.de)

The result of the phase calculation is a gray scaled image, which stands for a phase difference map between two subsequent acquired images. The gray value differences corresponding linearly to the displacement [4].

II. Experiments and results

The main source of that vibrations is expected to be the used chiller (ThermoTek ECO Serie, E900-16748, cooling efficiency 720 W – 900 W) and the used tubes consisting of polyamid. The very first step was to remove the chiller under the lab bench and placing it 3.5 m away, the maximum way due to the length of the cooling tubes. This is done to reduce the direct mechanical influence. After that, the noise is decreased from ±40 nm to ±34 nm, so all other measurements have been taken under these conditions.

A. CryLas beside Edgewave

In order to proof the mechanical noise of the laser chiller, a passively cooled Laser (CryLas FTSS355-50, 532 nm) is installed in the setup. The formerly used Edgewave laser was placed besides the CryLas without being operated, in order to determine the influence of the chiller and its vibrating case. If the Edgewave lasers' cooling is switched off and there is no water flow, the measurements performed with the CryLas were reliable with a variance of only ±1.2 nm. If the Edgewave chiller is switched on, there is a degradation to ±19.7 nm and even higher (up to ±32 nm) if the tubes from the Edgewave chiller are in contact to the CryLas. The results are displayed in Fig. 2. To avoid these effects, the vibrations of the chiller have to be eliminated and prevented from transferring to the lab bench. In this measurement, it could be shown that the vibrations and so the deteriorated images are mainly caused by chiller vibrations. That leaves three major problems to solve: First, the vibrations of the chiller case which are transferred via the ground to the lab

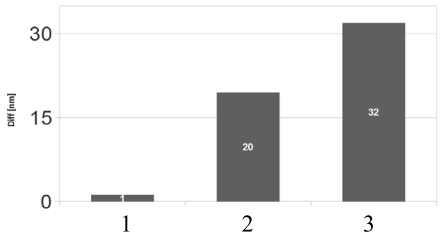

Fig. 2: CryLas besides Edgewave; 1: no cooling; 2: active Edgewave cooling; 3: contact between CryLas and cooling tubes from Edgewave

bench, second the ones which are transferred by the tubes and third the water flow inside the tubes itself.

B. Bypass at the cooling system

The first idea in order to eliminate the noise provided by the water flow, is to switch off the cooling process temporarily by the use of a bypass as shown in Fig. 3. A short time bypass is possible because for the measurement, only a limited number of pulses is required. The cooling flow is interrupted for five seconds, which is reasonable for the laser. The measurement is taken within this time.

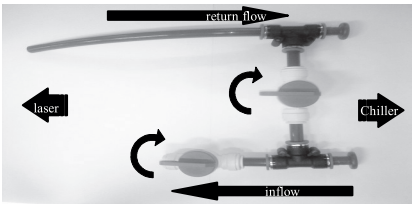

Fig. 3: Bypass at the cooling system, by turning the two screws, the inflow to the laser is interrupted

The first with cooling and the second with active bypass. As illustrated in Fig. 4, the active bypass deteriorates the results.

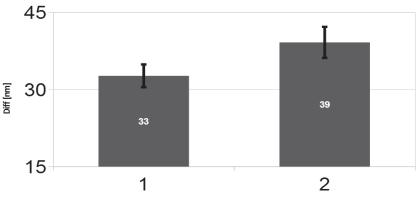

Fig. 4: Difference in nanometer at active cooling system(1) and without(2)

If the cooling system is interrupted, the laser loses thermal equilibrium and changes the beam profile. So this idea has to be rejected. The next step is to adjust the cooling system.

C. Different pressures in the cooling system

The second idea is to reduce the vibrations inside the tubes by decreasing the flow rate and the pressure. Inside the chiller case, there is an internal bypass which regulates the pressure and flow rate in the cooling system. These settings can be changed by an internal bypass screw. From the default position, it was turned clockwise and counterclockwise by three half turns, where a turn clockwise means to raise the pressure and a turn counterclockwise to lower the pressure.

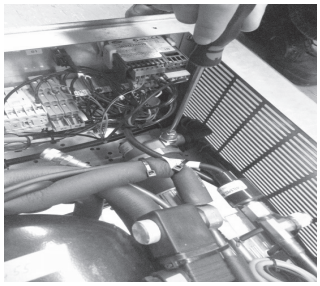

Fig. 5: Internal bypass screw

Several measurements under these different conditions have been taken. To monitor the changes, a pressure gauge has been installed into the system which shows not only the current pressure but also the flow rate. It was installed at the exit of the chiller in the inflow to the laser. The return flow has been unmodified.
While the setting of the internal bypass screw is changed, the flow rate and pressure is displayed on the pressure gauge. If the pressure is changed, the cooling rate has to be adjusted to keep the laser head on a constant temperature. The settings are summarized in Table I.

TABLE I
DIFFERENT OPERATING POINTS AND ASSOCIATED SETTINGS

Positions [turns]	Pressure [bar]	Flow [l/min]	Temp. Setting Laser Head [°C]	Temp. Setting Chiller [°C]
0	3,5	6,0	29,12	26,1
- 3/2	1,2	5,0	29,12	25,4
+3/2	4,8	7,0	29,12	26,2
- 1/2	2,7	5,8	29,07-29,12	25,8
+1/2	4,0	6,2	29,12	26,1
- 1/4	3,0	5,9/6,0	29,12	26,0

The received results are not significantly better for any setting, as one can see in Fig. 6. The results still vary from ±21 nm to ±29 nm. That has be the consequence of other effects, because the results are independent of the direction of screw turning. Consequently the stability cannot be improved by changing the pressure of the cooling water flow. This might be caused by the higher effort of the chiller, which becomes necessary because of the adjusted flow. So the vibrations in the tubes are lower, but the chiller itself has to work harder and the whole case has a higher vibration. Therefore there is no significant benefit in the measurement.

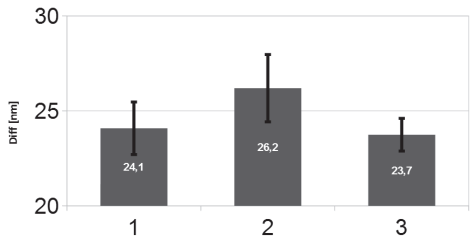

Fig. 6: 1: with higher pressure; 2: initial pressure; 3: lower pressure.

D. Different tube routing and manual damping

If the vibrations cannot be reduced by changing the pressure in the tubes, maybe the kind of tube routing has an influence to the vibrations and their transfer to the lab bench. For that reason three different tube positions were tested (Fig. 7). In addition, the tubes are held with both hands, which can alternatively be performed by a permanently installed damping.

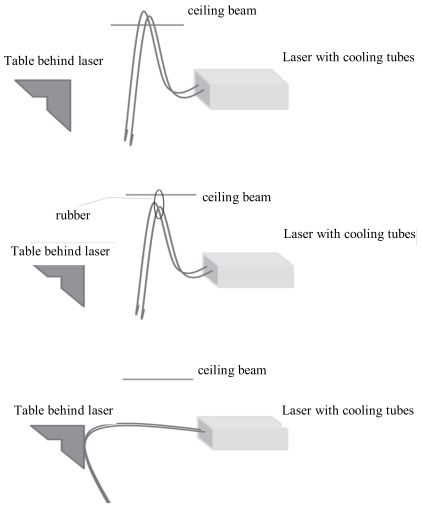

Fig. 7: (a) tubes at the ceiling; (b) tube in rubber at ceiling; (c) tubes from behind

As one can see in Fig. 8, the result while guiding the tubes at the ceiling are of improved stability at ±20 nm. If the tubes additionally are in a rubber, there is no significant improvement. But if the tubes are not at the ceiling, going directly into the laser head, the noise is higher with approximately ±29 nm. So on their way up and down, the water in the tubes get the chance to reduce turbulent flow. At the first two measurements, also a manual damping was tested by holding the tubes at two different positions. The noise level can be improved to ±14 nm.
It has been shown that the kind of tube routing improves the situation but it is still not suitable for reliable interferometrically measurement.

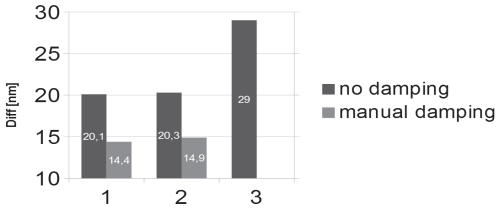

Fig. 8: Results to different tube positions shown in Fig. 7

E. Different tube types

For further reduction of the vibrations, a closer examination of the tubes is required. The delivered tubes made of polyamid are very rigidly and transfer the vibrations of the chiller to the lab bench. The idea is to use more flexible tubes and some with a higher inner diameter to absorb the turbulent flow which maybe induced vibrations, too. In addition, the inflow to the laser has been extended so that the water has the chance to release some of its vibrations.
Therefore two different types of tubes were tested. One with an inner diameter of 16 mm, and another with an inner diameter of 8 mm but also appreciably more flexible. In both cases the instability could be significantly lowered (Fig. 9).

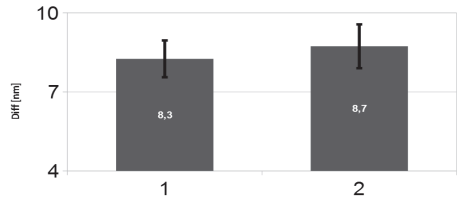

Fig. 9: series of four measurements, both tubes with higher flexibility; 1: inner diameter of 16mm; 2: inner diameter of 8mm

In average, there is a difference of 8.5 nm ± 1.4 nm. To improve further stability, a heat exchanger is installed additionally, which is expected to be useful due to the small water channels which could lower high frequency pressure waves within the water flow. It stabilized the water flow and reduces so the transformable high frequency vibrations. This further improves the noise of two nanometers to 6.5 nm.

F. Dumping laser head with synthetic material

For further reduction of noise, the laser head itself can be dumped. Therefore, it was underlaid with synthetic material to avoid that little vibrations which occur direct in the laser head have an effect on the optical elements on the lab bench (Fig. 10).

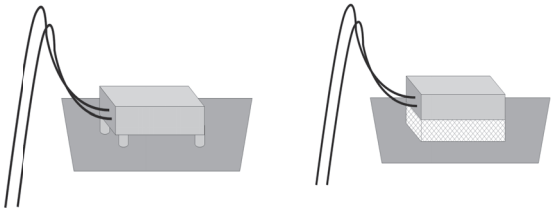

Fig. 10: left: Laser firmly attached to lab bench; right: Laser decoupled and underlaid with synthetic material.

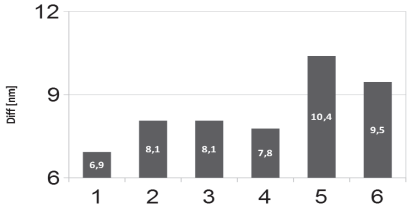

Fig. 11: results of decoupled laser

As shown in Fig. 11 the difference in nanometers is 8.4 nm ±1.2 nm. So the decoupling of the laser does not improve the stability. Furthermore, the adjustment of the laser head is more difficult.

III. Discussion

The three main reasons for vibrations and therefore unreliable phase measurements are the chiller case vibrations transferred by the ground as well as the water tubes plus the irregular water flow. All have been reduced by mechanical interventions. One can see that the tubes and as a consequence thereof the water flow inside have a large influence. If the tubes are changed to some with higher inner diameter there is an improvement of more than ten nanometers. The change of pressure and flow rate as well as the laser head dumping are not improving the results. A bypass in the cooling system is not useful because it has been shown that the results became even worse if the cooling system is interrupted due to temperature change in the laser head. The reason for the still lower stability in the new setup compared to the first one is expected to be the type of the water pump in the cooling system, which is not capable of providing a constant flow. The use of a centrifugal pump would be an alternative. But this pump has also some disadvantages, for example the lower efficiency which will lead to a more vibrating case.
In conclusion the instability could be lowered to a level which is sufficient reliable to start photoacoustic measurement, even if the vibration is still higher compared to the old setup.

IV. References

[1] Horstmann, J. and Brinkmann, R.: “Non-contact photoacoustic tomography using holographic full field detection.” , vol. 8800, pp. 880007-880007-6, 10.1117/12.2033599
[2] Carp, S. A., Venugopalan, V.: “Optoacoustic imaging based on the interferometric measurement of surface displacement”, J. Biomed. Opt. 12(6), 064001 (December 19, 2007). doi:10.1117/1.2812665
[3] Helmers H., Burke J., “Performance of spatial vs. temporal phase shifting in ESPI”, Proc. SPIE 3744, 188-199 (1999).
[4] Pedrini, G., Pfister, B., Tiziani, H., "Double pulse-electronic speckle pattern Interferometry," Journal of Modern Optics, 40 (1), 89-96 (1993)

Implementation of a reconstruction algorithm for Photoacoustic Tomography

M. Münter, C. Buj, J. Horstmann and R. Brinkmann

***Abstract*—Photoacoustic Imaging has become increasing popular in recent years. It is a non-ionizing imaging-technique with high potential in medicine, especially suited to image the vascular system. This paper is based on a full-field surface detection system by interferometry. Therefore an absorber detection by mathematical time reversal reconstruction is needed. In this paper, the results of a two-dimensional delay-and-sum reconstruction algorithm for different sizes of point absorbers are presented, which have been done by Matlab. It has been shown that the two dimensional reconstruction is reliable for spherical absorbers.**

I. Introduction

Photoacoustic Imaging is a tomographic technique, which combines the advantages of light and ultrasound. It is based on the photoacoustic effect, shown schematically in Fig. 1. The absorption of electromagnetic radiation is followed by temperature increase in the absorber, which results in a rising pressure in the absorber. This causes in thermoelastic expansion and pressure wave emission.

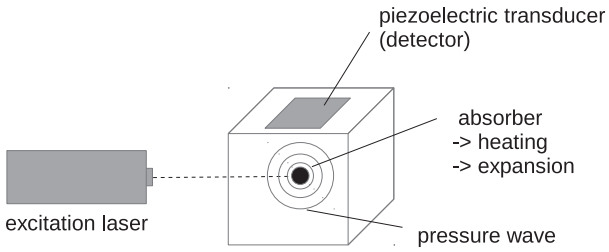

Fig. 1. Schematic representation of the photoacoustic effect

State-of-the-art limitations are a long acquisition time and the need for acoustic contact, such as the use of a piezoelectric sensor system to detect the pressure waves [1]. Fig. 2 introduce a novel non-contact full-field approach by the Medical Laser Center Luebeck [2] for Photoacoustic Tomography. The detection system consists of a Mach-Zehnder interferometer and a

M. Münter, Medizinische Ingenieurwissenschaft, Universität zu Lübeck; the work has been carried out at the Institute of Biomedical Optics, Universität zu Lübeck, Luebeck, Germany (e-mail: muenter@miw.uni-luebeck.de).

C. Buj is with the Institute of Biomedical Optics, Universität zu Lübeck, Luebeck, Germany (e-mail: buj@bmo.uni-luebeck.de).

J. Horstmann is with the Medical Laser Center Luebeck GmbH, Luebeck, Germany (e-mail: horstmann@bmo.uni-luebeck.de).

R. Brinkmann is with the Institute of Biomedical Optics,Universität zu Lübeck, Luebeck, Germany and the Medical Laser Center Luebeck GmbH, Luebeck, Germany (e-mail: brinkmann@mll.uni-luebeck.de).

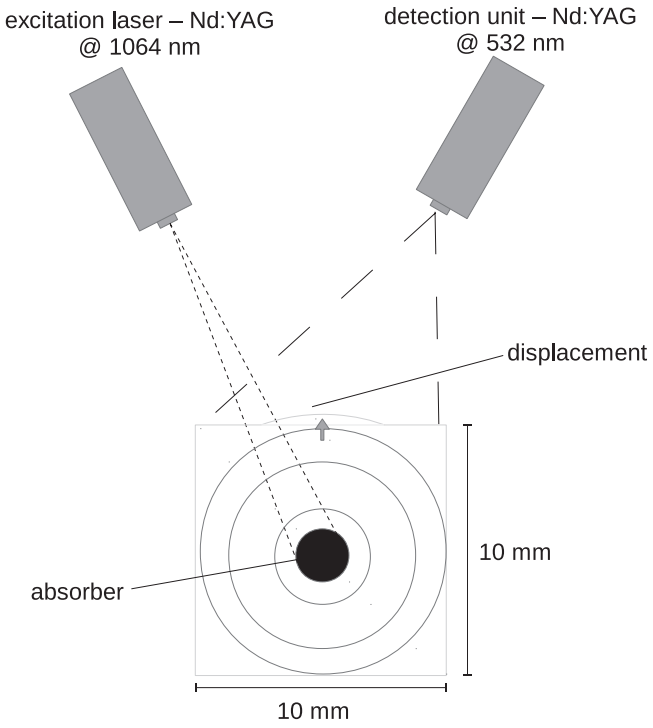

Fig. 2. Holographic Photoacoustic Imaging. Excitation pulses are applied to the volume. The pressure induced surface displacements owing to thermoelastic expansion of absorbers are recorded by an optical-holographic detection unit.

high-speed CCD-camera (Basler Pilot piA1600-35g), which captures the object and reference beam from the detection laser with a frame rate of 20 Hz. The detection laser (CryLas FTSS 355-50, pulse duration 1 ns) is a frequency doubled Nd:YAG laser with a wavelength of 532 nm. For excitation a flashlamp pumped Nd:YAG (Quantel YG571C, pulse energy 25 mJ, spot size 5 mm, repetition rate 10 Hz) laser is used with a pulse duration of 6 ns and a wavelength of 1064 nm. The detection of surface deformations is based on the principle of Electronic Speckle Pattern Interferometry (ESPI), a method for measuring very small changes in distances in nm range [3], [4]. In order to calculate the position of the absorber, a appropriate reconstruction method must be implemented.

II. Material and Methods

The mathematical software programming language Matlab (Mathworks) is used, to develop an algorithm for two-dimensional reconstruction and to visualize the first concepts.

An adjusted delay-and-sum algorithm on the basis of the work of Carp & Venugopalan [5] and Hoelen & du Mul [6] is implemented to reconstruct the position of the acoustic sources after data acquisition. The sequences of the algorithm are schematically visualized in Fig. 3. Due to hardware limitations,

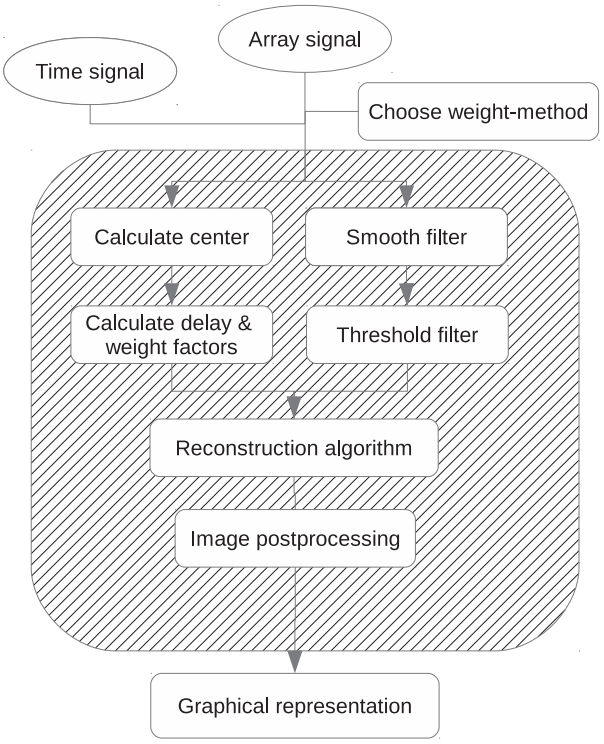

Fig. 3. Flow chart of the Photoacoustic Imaging program, based on the delay-and-sum principle.

an equidistant data acquisition was not possible. For this reason, the missing data was interpolated with a shape-preserving cubic interpolation algorithm for better results . To minimize the influence of noise of the measured data, a 4x4 Gaussian filter was applied. Furthermore, to remove background noise, a simple threshold filter was used to extract artefacts. The threshold filter extracted the values, who are less than 90 % of the maximum intersection value.

A. Principle of triangulation

The approach is based on the principle of triangulation. When the time of surface displacement and the velocity of the spherical wave are known, the location of the absorber can be calculated.

$$c = \frac{m}{t} \rightarrow m = c \cdot t, \tag{1}$$

where m is the distance from the absorber to the detection layer, t the time from absorption to detection and c the velocity of the sound wave. The propagation velocity of the acoustic wave in the silicone phantom is measured to be approximately $830\frac{m}{s}$ to $1050\frac{m}{s}$. The varying of the velocity is caused by the hardening of the silicone. For example, there are three sensors detecting a spherical wave from an unknown source at different times t_1, t_2, t_3. The radius (calculated distances m_1, m_2, m_3) of the circles make up the possible sources of the spherical wave. If there are at least three sensors in two dimensions, a definite source can be predicted at the point of intersection. In addition, depending on the distance to the center of the spherical wave, the calculated places of origins were attenuated with a weighting factor w, which is calculated through a Gaussian function.

B. Phantom

The two-dimensional reconstruction is used for a phantom, consisting of three components. A black-stained silicone ball (absorption coefficient $= 29.6cm^{-1}$ for $\lambda = 1064nm$), who serves as an absorber, is stored in a transparent silicone cuboid. The area, which is sampled is coated with a white thin silicone layer, in order to enable a better detection.
The absorber is usually located in $5mm \pm 1mm$ depth below the detection surface. The size of the entire cuboid is $10\text{x}45\text{x}10mm$ (height, width, depth), shown in Fig. 4.

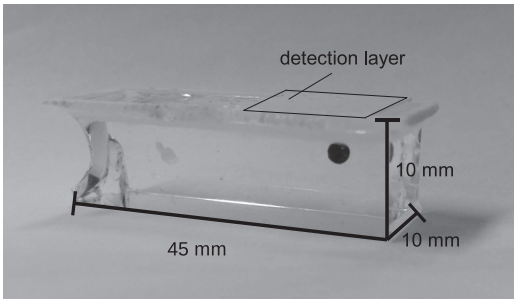

Fig. 4. Silicone phantom with a black-stained silicone ball in the center

The high-speed-camera records an image with a resolution of $1200x1600$ pixels, whereby a pixel correlates to $7.4\mu m$. Therefore, an area of 8.88 mm x 11.74 mm is captured with an imaging scale of 1:1. Fig. 5 shows 6 representative images at different time steps of the surface deformation, which was induced by the spherical pressure wave. The gray values can

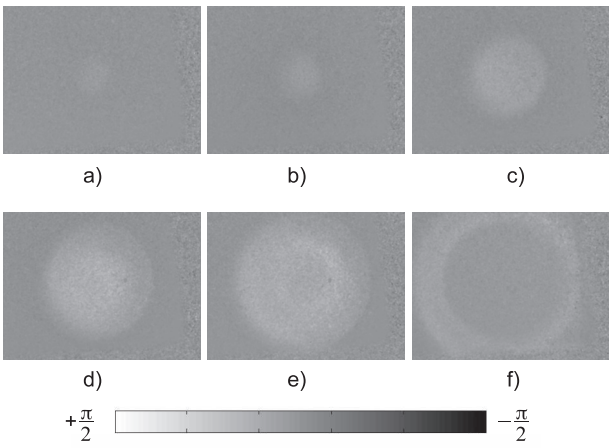

Fig. 5. Phase difference images at different time steps, relative to the point of excitation a) 4,618 μs b) 4,760 μs c) 5,246 μs d) 5,801 μs e) 6,334 μs f) 7,568 μs

be converted into nanometre scale from $-\pi/2$ to $+\pi/2$. For the two-dimensional reconstruction a line from the data over time was extracted, as shown in Fig. 6.

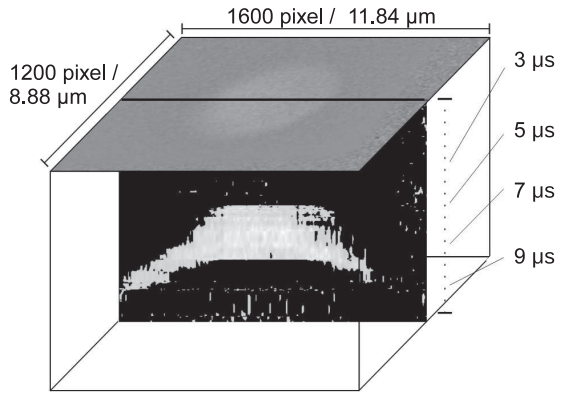

Fig. 6. Extracted sensor line with captured surface deformation

Depending on the position of a pixel and the corresponding measured time, when the spherical wave is measured, a circle is stored in an array. The occurred intersections provide the position and form of the reconstructed absorber.

III. Results and Discussion

Two-dimensional images of two absorbers with different diameter were reconstructed, to show the abilities of the delay-and-sum-algorithm. The images were taken at 114 different time steps for a 2 mm point absorber and for a 1 mm absorber at 168 time steps. Furthermore, the images were interpolated to 0.01 μs steps from 0 μs to 1000 μs. A line segment above the absorber were taken for reconstruction. Fig. 7 shows the reconstructed image without a threshold filter and points out the impact of ring artefacts due the art of reconstruction. To reduce these artefacts, the results were threshold filtered, shown in Fig. 8.

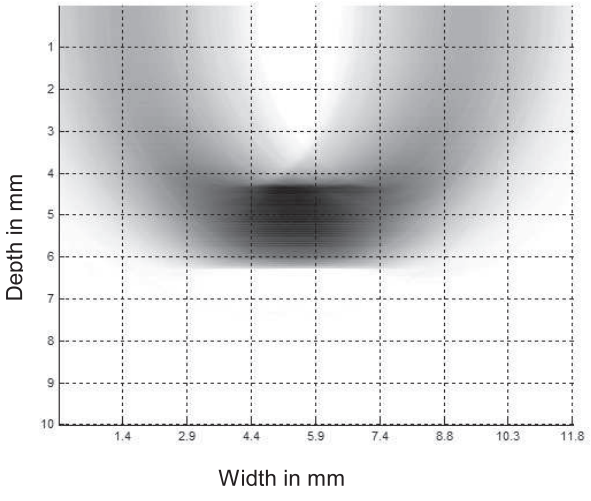

Fig. 7. Reconstructed image from 2 mm absorber without threshold filter

In the reconstruction the first 2 mm absorber is located in 4.2 mm depth with a reconstructed diameter of 1.7 mm. As Fig. 8 visualizes, the largest probability of presence of depth is 5 mm.

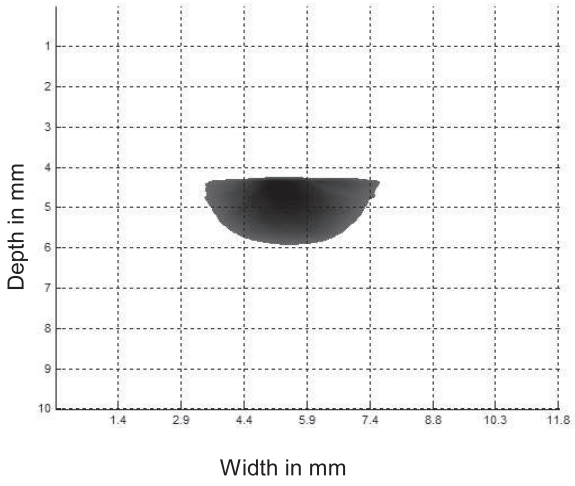

Fig. 8. Reconstructed 2 mm absorber with $c = 830\frac{m}{s}$

The 1 mm absorbers is located in 4 mm depth and has a reconstructed diameter off 1.2 mm.

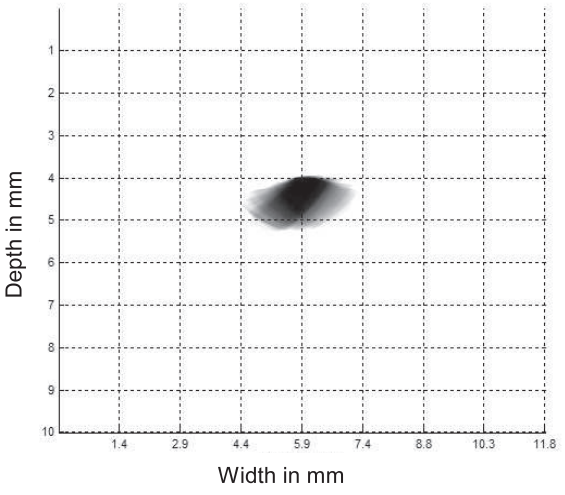

Fig. 9. Reconstructed 1 mm absorber with $c = 1054\frac{m}{s}$

The results are concluded in Table I. The algorithm has also been tested for the reconstruction of two absorbers, shown in Fig. 10. When the displacement of the first sound wave of the first absorbers propagates, the second wave arrives and interferes with the first one.

TABLE I
Measured and reconstructed diameter and depth

Absorber	rec. Diameter	meas. depth	rec. depth
1 mm	1.2 mm	4 mm	4 mm
2 mm	1.7 mm	4.2 mm	4.3 mm

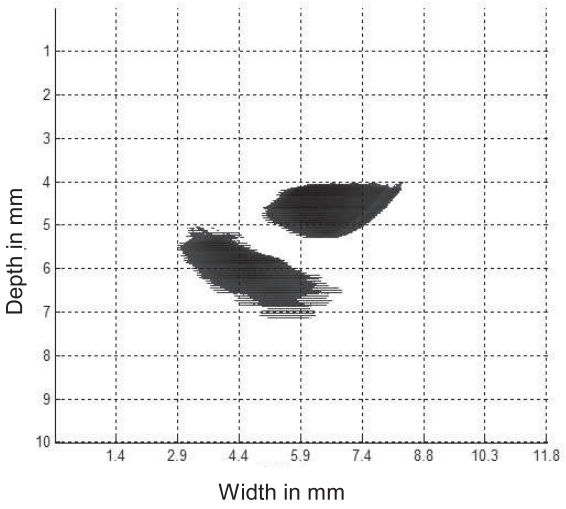

Fig. 10. Reconstructed image of two point absorbers

IV. Conclusion

In this paper, a two-dimensional reconstruction for the non-contact photoacoustic imaging setup of the Medical Laser Center Luebeck was developed. The 1 mm absorber, in comparison to the 2 mm absorber, has a more spherical shape and also provides more accurate values for diameter and depth. In addition, the maximum of all intersections for the 1 mm absorber was at a depth of 4.5 mm, which corresponds to the depth of the phantom. A first estimate about the depth can be determined relatively precisely, but is caused by varieties by the different values of propagation speed. Additionally, the shape and diameter can only be assumed, which is unavoidable due to the art of reconstruction.

A. Outlook

On the one hand, a nearly exact depth and diameter of the absorber could be found, so that the type of reconstruction was sufficient for the initial phase of the project. On the other hand, more proved reconstruction methods [7] could be investigated. Especially the statistical analysis about depth, shape and diameter in comparison to established tools, like optical coherence tomography should be treated and could help to evaluate the quality of the reconstruction by triangulation in detail. In the further course, the behaviour in the medium to the absorber should be more investigated to improve the reconstruction results. In particular, different types of absorbers, shapes, structures should be measured.

References

[1] M. Xu and L. V. Wang, "Photoacoustic imaging in biomedicine" *Review of Scientific Instruments*, vol. 77, no. 4, pp. 041101 - 041101-22, Apr. 2006 .

[2] J. Horstmann and R. Brinkmann, "Non-contact Photoacoustic Tomography using holographic full field detection", *Proc. of OSA-SPIE*, vol. 8800, pp. 880007-1, 2013.

[3] R. Büttner, "Untersuchung und Aufbau eines Laser-Speckle-Abstand- und Geschwindigkeitssensors", dissertation, Ernst-Moritz-Universität Greifswald, Institut für Physik , 2008 .

[4] H. Helmers and J. Burke, "Performance of spatial vs. temporal phase shifting in ESPI", *Proc. SPIE*, vol. 3744, pp. 188-199, 1999.

[5] S. A. Carp and V. Venugopalan, "Optoacoustic imaging based on the interferometric measurement of surface displacement" *Journal of Biomedical Optics*, vol. 12, no.6, pp. 064001, Nov./Dec. 2007 .

[6] C. A. Hoelen and F. F. M. de Mul, "Image reconstruction for photoacoustic scanning of tissue structures", *Applied Optics*, vol. 39, no. 31, pp. 5872-5883, 2000 .

[7] M. Xu and L. V. Wang, "Universal back-projection algorithm for photoacoustic computed tomography", *Phys. Rev. E*, vol. 71, no. 1, pp. 016706-1 - 016706-7, 2005 .

Light transmission measurements and beam size quantification in porcine eyes

J. Rehra, A. Baade, K. Schlott, and R. Brinkmann

***Abstract*—Laser photocoagulation is a leading treatment in a range of retinal diseases. Besides the therapeutic effects, every treatment produces an irreversible impairment of the neural retina which should be as low as possible. The beam diameter at the fundus as well as the light transmission through the eye influence the appearance of the lesion as well as the accuracy of the non-invasive temperature measurement. In this work, a special holder for porcine eyes that minimizes the deformation of the eye was designed and constructed. Using this holder, measurements to determine the transmission and the beam diameter at the fundus were performed for a wavelength of 532 nm. The transmission through porcine eyes was found to be 86 %, measured behind a 4 mm-hole in the central fundus, the beam diameter was found to be in good agreement with the setting selected at the slit lamp.**

I. Introduction

The treatment of retinal diseases by *photocoagulation* is being performed since the 50s of the last century. The first applications were done with focused sunlight by Meyer-Schwickerath [1], although the development of the *Laser* in the 1960s enabled the real breakthrough of the technique [2]. Until today, the laser-photocoagulation is a leading standard in the treatment of a range of retinal diseases such as macular edema and the diabetic retinopathy [3], [4].

The therapeutic effect of photocoagulation is based on thermal damaging of the retina by absorption of light. The *retinal pigment epithelium* (RPE) is rich in the pigment melanin which has a high absorption coefficient in the range of visible light. Absorbed light is transduced into heat by internal conversion which leads to a temperature rise in the surrounding tissue. Proteins in the adjacent tissue are denatured if a temperature threshold is reached, producing a small area of necrosis. Nowadays, green light emitting lasers are commonly used for coagulation due to a reasonable compromise between a low diffusion in the sclera and a high absorption in the RPE [4].

Beside the positive effects, every application of intense light produces a non-reversible impairment in the eye which should be as low as possible without losing its clinical effect. It is desired to produce a lesion just above the limit of damaging, independent of the conditions of the treated fundus and other influencing factors. However, a wide range of variations, e.g. pigmentation of the fundus, is found even in the same eye. This poses difficulties in the dosage of the laser power for the ophthalmologist.

The decisive factor for the effect of the coagulation is the temperature reached in the ocular fundus. *Optoacoustics*, beside other approaches as reflectometry, magnetic resonance imaging and optical coherence tomography, looks the most promising concerning a practically relevant real-time measurement of the temperature in the fundus of a patient during treatment [5]. Using the *optoacoustic effect*, the light energy of a short laser pulse can be transformed into acoustic energy. The absorption of light in a tissue causes a temperature rise, depending on the properties of the tissue and the parameters of the laser. This temperature rise leads to an expansion of the affected tissue. If the deposed energy per pulse is high enough within a short time (*thermal confinement time*), each laser pulse produces a bipolar pressure wave propagating through the tissue as an ultrasonic wave. Measuring these ultrasonic wave, the temperature in the laser focus can be determined after a calibration with a known temperature [6].

The project “Automatic Photocoagulation of the Retina” (AutoPhoN) at the Medical Laser Center Lübeck GmbH (MLL) uses this optoacoustic method to realize an online dosimetrie during treatment of the ocular fundus. For that application, a second probe laser is coupled into the beam path of the treatment laser. It repeatedly measures the temperature with nanosecond pulses. Surveilling the temperature profile during treatment, the treatment laser can be stopped when reaching a predefined temperature, corresponding to the desired coagulation [5].

The exact calculation of the temperature depends on a set of parameters as described in [6], [7]. The beam diameter and profile have a great bearing on the calculation and have to be known correctly, as well as the exact power applied to the fundus which is influenced by absorption in the setup and the ocular media. In this work, the beam diameter at the back of the eye was investigated. The experiments are performed on enucleated porcine eyes, fixed in a newly designed eye holder. As a deformation of the eye can lead to distortion of the laser beam and therefore to inaccuracies in the temperature calculation, the eye is nearly completely enclosed by the holder to prevent deformation.

II. Material and Methods

A. Eye holder and basic setup

The eye holder is designed using SolidWorks and manufactured in the mechanical workshop of the Universität zu Lübeck.

J. Rehra, Medizinische Ingenieurwissenschaft, Universität zu Lübeck, the work has been carried out at Medical Laser Center Lübeck, (e-mail: rehra@miw.uni-luebeck.de).

A. Baade is with Medical Laser Center Lübeck (telephone: +49 (0)451 500 6521, e-mail: baade@mll.uni-luebeck.de).

K. Schlott is with Medical Laser Center Lübeck (telephone: +49 (0)451 500 6417, e-mail: schlott@mll.uni-luebeck.de).

R. Brinkmann is with Medical Laser Center Lübeck and with Institute for Biomedical Optics, Universität zu Lübeck (telephone: +49 (0)451 500 6507, e-mail: brinkmann@bmo.uni-luebeck.de).